SHADOWGRAPHY OF THE END-EFFECTS REGIME PRODUCED BY CLUSTERED ROCKETS

Andres Canchero[1], Raymundo Rojo[1], Charles E. Tinney[1], Nathan Murray[2] & Joseph H. Ruf [3]
[1]*Aerospace Engineering & Engineering Mechanics, The University of Texas at Austin, Austin, USA*
[2]*National Center for Physical Acoustics, University of Mississippi, University, USA*
[3]*NASA Marshall Space Flight Center Huntsville, Alabama, USA*

Abstract The plume produced by a cluster of two high area-ratio thrust optimized parabolic contour nozzles is visualized by way of retroreflective shadowgraphy. Both steady and transient operations of the nozzles (start-up and shut-down) were conducted in the anechoic chamber and high speed flow facility at The University of Texas at Austin. Both nozzles exhibit free shock separated flow, restricted shock separated flow and an end-effects-regime prior to flowing full. Radon transforms of the shadowgraphy images are used to identify the locations in the flow where sound waves are being generated. During these off design operations of the nozzles, most sound waves are generated by turbulence interactions with the shock cells located in the supersonic annular plume. During the end-effects-regime, this supersonic annular plume is shown to flap violently, thus providing a first principals understanding of the sources of most intense loads during engine ignition.

MOTIVATION

In this study, two high area-ratio rocket nozzles comprising TOP contours are placed side by side and are examined during a single start-up followed by several steady state operations. The objective of the effort is to better understand the acoustic environment produced by clustered rocket engines and how these environments relate to the flow patterns that form inside TOP rocket nozzles during ignition. While the flow field is more readily accessible using numerical methods (such as Reynolds-averaged Navier-Stokes or large eddy simulation), or by leveraging visualization techniques (such as Schlieren, shadowgraphy and even particle image velocimetry), the acoustic environment is less known, and more difficult to predict. A large part of the challenge resides with the non-stationary operations of the nozzle and rocket plume during ignition. Here, we will synchronize visuals of the rocket exhaust and shock foot locations with acoustic waveforms measured behind the nozzles (where the base of the vehicle would reside) during start-up. While much of our previous emphasis has been on single nozzle configurations [1, 2, 3], the current study will employ two nozzles operating at nearly identical nozzle pressure ratios. Such a configuration is a more realistic representation of the full scale operating environment.

EXPERIMENTAL DESCRIPTION

All measurements reported here were conducted in the anechoic chamber and high speed flow facility at The University of Texas at Austin. A description of the facility is provided elsewhere [2, 3] and includes a nozzle test stand located at the center of a fully anechoic chamber and open jet wind tunnel. The test hardware comprised two thrust-optimized parabolic (TOP) contour nozzles with one nozzle located directly above the other. Both nozzles are geometrically identical and comprise a throat radius of r^* = 6.35 mm (0.25 in) and an exit-to-throat area ratio of A_e/A^* = 30.29. The design Mach number is thus 5.24 and can be achieved with a nozzle pressure ratio (NPR, the ratio of plenum pressure to atmospheric pressure) of approximately 700.

Three unique instruments were used for this study. That is, a eighth-inch microphone, a sixteen channel static wall pressure sensing array and a shadowgraphy system. Given both the temporal resolution afforded by the microphone system and the non-stationary operation of the nozzle during start-up, a time-frequency analysis of the microphone data is conducted in order to view the spectral content as function of time (or NPR). In particular, the Morlet wavelet transform is employed with a description of its implementation to jet and rocket noise studies being provided by Baars & Tinney [2] and Donald *et al.* [3]. As for the static wall pressure inside each nozzle, this was recorded using two Scanivalve DSA3218 gas pressure scanners in order to provide an understanding of the shock foot wall pattern for a given nozzle pressure ratio. The third instrument comprised a retro-reflective shadowgraphy system in order to visualize the exhaust plume and acoustic field. Direct shadowgraphy detects sharp refractive disturbances (e.g. strong velocity gradients, shock waves and high amplitude sound waves) as it visualizes the Laplacian of the refractive field [5, 6, 7]. The current set-up is similar to the one used by [4].

Sample images from the shadowgraphy system are shown in figure 2 at NPR 30, 37 and 70. FSS to RSS transition occurs at NPR 24.4 for this nozzle contour while the end effects regime initiates around NPR 37. The end effects regime is known to produce the most intense source of vibro-acoustic load during start-up. Here is it is visualized in figure 2(b) and

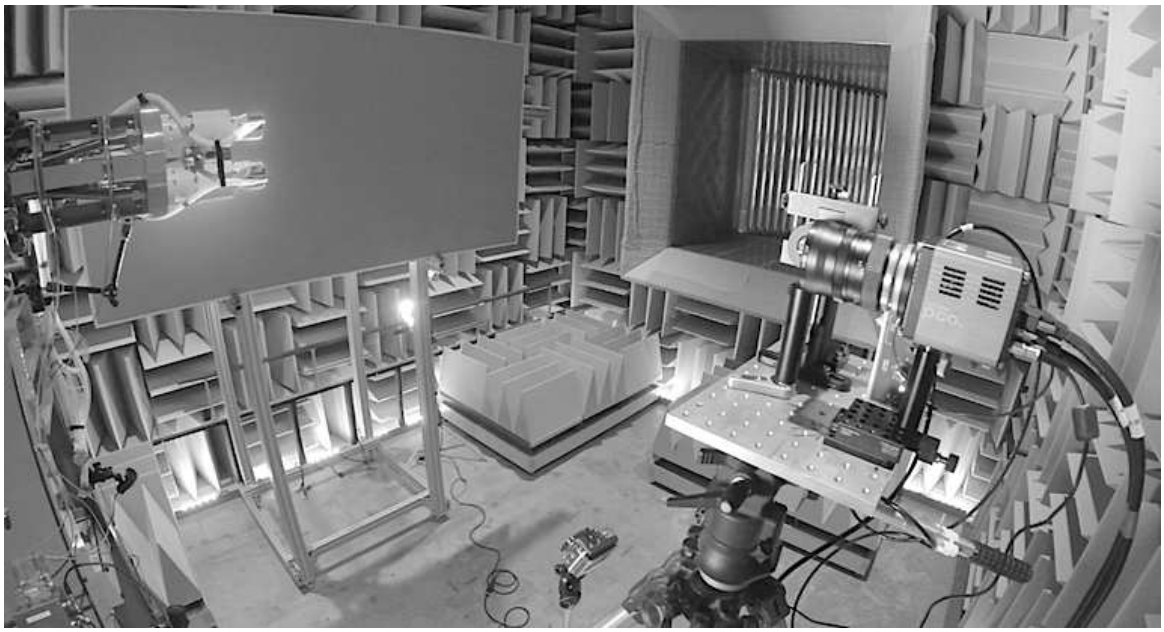

Figure 1. Arrangement of optical components relative to the nozzle test stand.

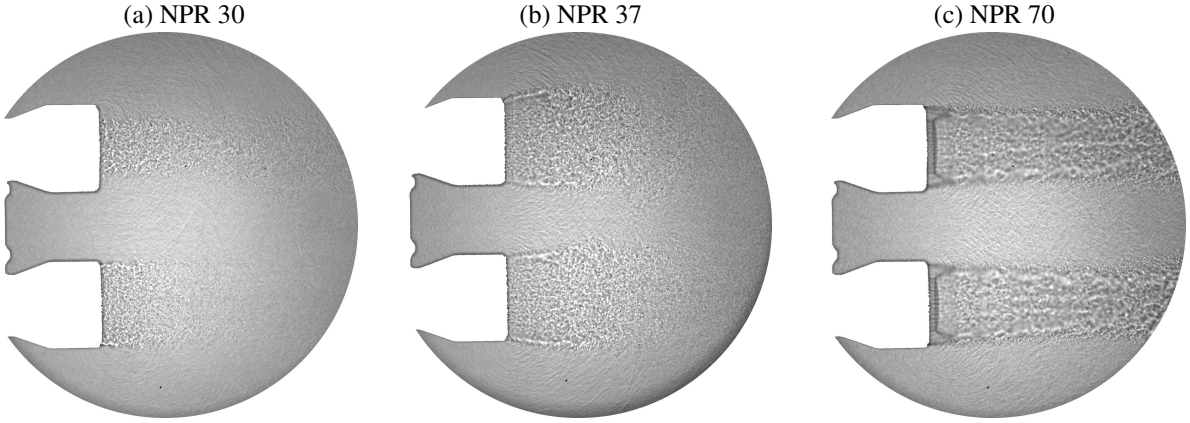

Figure 2. Shadowgraphy images of the instantaneous rocket plumes during non-stationary start-up at (a) 30, (b) 37, (c) 70.

is shown to be the consequence of severe radial spreading of the supersonic annular shear layer. This spreading occurs when the last trapped annular separation bubble opens intermittently to the atmosphere.

References

[1] W. J. Baars, J. H. Ruf, and C. E. Tinney. Non-stationary shock motion unsteadiness in an axisymmetric geometry with pressure gradient. *Experiments in Fluids*, **56**(92), 2015.

[2] W. J. Baars and C. E. Tinney. Transient wall pressures in an overexpanded and large area ratio nozzle. *Experiments in Fluids*, **54**(2), 2013.

[3] B. Donald, W. Baars, C. Tinney, and J. Ruf. Sound produced by large area-ratio nozzles during fixed and transient operations. *AIAA Journal*, **52**(7):1474–1485, 2014.

[4] M. J. Hargathar and G. S. Settles. Retroreflective shadowgraph technique for large scale flow visualization. *Applied Optics*, **48**(22), 2009.

[5] W. Merzkirch. *Flow Visualization*. Academic Press, 2nd Edition, 1987.

[6] G. S. Settles. *Schlieren and Shadowgraph Techniques*. Springer-Verlag, 2001.

[7] C. Tropea, J. F. Foss, and A. L. Yarin. *Springer Handbook of Experimental Fluid Mechanics*. Springer-Verlag, 2007.